

Depicting Beyond Scores: Advancing Image Quality Assessment through Multi-modal Language Models

Zhiyuan You^{12*}, Zheyuan Li^{2*}, Jinjin Gu^{34*}, Zhenfei Yin³⁴,
Tianfan Xue^{14†}, Chao Dong^{24†}

¹The Chinese University of Hong Kong,

²Shenzhen Institute of Advanced Technology, Chinese Academy of Sciences,

³University of Sydney, ⁴Shanghai AI Laboratory

zhiyuanyou@foxmail.com zheyuanli884886@gmail.com jinjin.gu@sydney.edu.au
zyin7056@uni.sydney.edu.au tfxue@ie.cuhk.edu.hk chao.dong@siat.ac.cn

Abstract. We introduce a **Depicted** image **Quality Assessment** method (DepictQA), overcoming the constraints of traditional score-based methods. DepictQA allows for detailed, language-based, human-like evaluation of image quality by leveraging Multi-modal Large Language Models (MLLMs). Unlike conventional Image Quality Assessment (IQA) methods relying on scores, DepictQA interprets image content and distortions descriptively and comparatively, aligning closely with humans' reasoning process. To build the DepictQA model, we establish a hierarchical task framework, and collect a multi-modal IQA training dataset. To tackle the challenges of limited training data and multi-image processing, we propose to use multi-source training data and specialized image tags. These designs result in a better performance of DepictQA than score-based approaches on multiple benchmarks. Moreover, compared with general MLLMs, DepictQA can generate more accurate reasoning descriptive languages. Our work demonstrates the utility of our full-reference dataset in non-reference applications, and indicates that language-based IQA methods have the potential to be customized for individual preferences.

Keywords: Image Quality Assessment · Multi-modal Language Models

1 Introduction

Image Quality Assessment (IQA) is an important and challenging topic in low-level vision research. IQA aims to measure and compare the quality of images, expecting the final results to be aligned with human judgments. Existing IQA methods [15, 43, 55, 64] mainly output the quality or similarity scores, which have apparent shortcomings. First, image quality is affected by different factors that

* Contribute Equally. † Corresponding Author.

Project Page: <https://depictqa.github.io>.

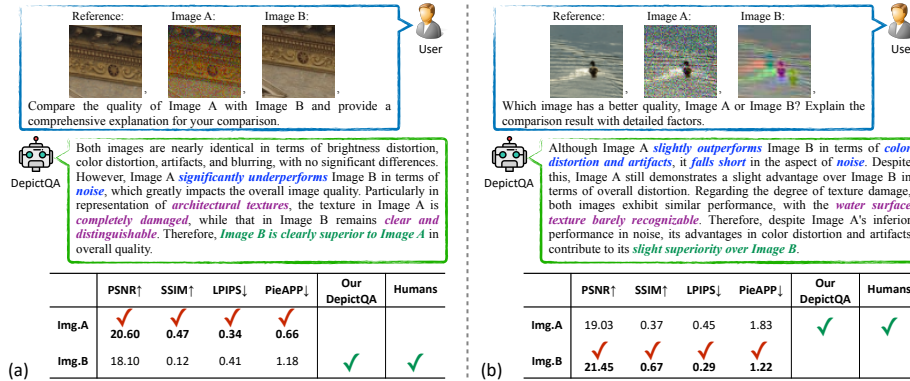


Fig. 1: Comparison between our Depicted image Quality Assessment method (DepictQA) and score-based Image Quality Assessment (IQA) methods, including PSNR, SSIM [55], LPIPS [64], and PieAPP [43]. Score-based IQA methods only provide numerical scores devoid of reasoning and justification. Thus they disagree with human judgments in complex scenarios when (a) images are misaligned and (b) both images suffer from severe distortions. In contrast, DepictQA first identifies the **distortions** of images, then weighs the influences of different distortions to the **texture damages**, and finally obtains the **comparison results** that are better aligned with human judgments.

cannot be effectively expressed by a simple score, *e.g.*, noise, color distortion, and artifacts in Fig. 1. Second, the reasoning process by humans cannot be well modeled by current IQA methods. For example, in Fig. 1b, humans may first identify the distortions (*i.e.*, noise in Image A, color distortion and artifacts in Image B), then weigh the impacts of these distortions on overall visual quality (color distortion and artifacts in Image B are worse than noise in Image A), and finally conclude that Image A is better than Image B. On the contrary, existing IQA methods simply compare the quality scores of these two images.

To better align with humans, we explore a new paradigm for IQA, named **Depicted image Quality Assessment** (DepictQA). Inspired by recent Large Language Models (LLMs) [36, 51] and multi-modal technologies [28, 70], we believe that language is the key to solving the above problems. As shown in Fig. 1, DepictQA takes both images and a question as inputs, then outputs a paragraph that describes the quality of images from multiple aspects. Furthermore, empowered by the reasoning capability of LLMs, DepictQA can weigh the importance of each distortion and make the final judgment. For instance, in Fig. 1a, DepictQA finds that “the texture in Image A is completely damaged” while “Image B remains clear and distinguishable”, thus concludes “Image B is superior to Image A”. Learning this kind of reasoning makes DepictQA better at aligning human judgments than existing methods in complex scenarios like misalignment (Fig. 1a) and multiple distortions (Fig. 1b). Meanwhile, these descriptive outputs can be naturally understood by humans, greatly improving the interpretability.

To integrate language into IQA, we establish a hierarchy of tasks, inspired by human evaluation. Humans first perceive the distortions of the image, then

use this information to determine the image quality. Also, it is easier for humans to compare the difference between two images in a single dimension (*e.g.*, color distortion) than quantitatively evaluate the overall quality of an image or the similarity between two images, as verified by [40, 42, 43]. Based on this intuition, DepictQA does not produce scores, but describes the image quality and compares two images. Specifically, we break DepictQA task into a hierarchy of 3 tasks (detailed in Fig. 2): (1) Quality Description, (2) Quality Comparison, and (3) Comparison Reasoning. These designs follow the process of human evaluation.

To train the proposed DepictQA, we further construct a multi-modal IQA dataset, named M-BAPPS, by collecting text descriptions based on the existing BAPPS IQA dataset [64]. Our M-BAPPS dataset contains 5,104 detailed high-quality text descriptions and 115,646 brief descriptions. For high-quality texts, we first collect the quality-related information through a carefully designed questionnaire (details shown in Fig. 2a and 2c), the results of which are further converted into a descriptive paragraph using GPT-4 [36]. To further increase the size of the training set, we also augment the dataset with brief descriptions. Specifically, we convert the existing quality comparison label in BAPPS into a brief description using pre-generated templated texts, such as “Image A maintains a distinct advantage in terms of image quality over Image B”.

With the dataset mentioned above, we resort to Multi-modal Large Language Models (MLLMs) [18, 28, 70] to bridge the gap between images and descriptive texts. However, directly applying existing MLLMs to our DepictQA faces two challenges. First, there are only limited images with high-quality descriptions, preventing the model from robustly correlating images and text descriptions. In this aspect, we present a multi-source training approach to increase the size of training data. Specifically, two additional sources are used. One is images with only brief templated texts, as mentioned above. The other one is external quality-unrelated content description data, the Detailed Description dataset in [61], which contains 48,734 image-text pairs. Although these two datasets are not directly designed for the descriptive reasoning ability, we find that the former one can help bridge images and texts in quality-related tasks, while the latter one can serve as a regularization. Second, many MLLMs have difficulty in distinguishing multiple images, but our setup requires two or more images. We solve this problem by employing specialized tags for different images, instead of a unified tag for all images. Empirical results demonstrate that these approaches effectively mitigate the two challenges and bring a better DepictQA model.

Finally, we conduct experiments to prove the effectiveness of DepictQA. First, DepictQA achieves state-of-the-art performance on the BAPPS benchmark, well aligned with human judgments. Also, DepictQA can describe the distortions and texture damages in images and explain the reasoning process when comparing two images, thus generating more accurate descriptions compared with general-purpose MLLMs. Even compared with notably GPT-4V [37], DepictQA has significantly better comparison ability and comparable reasoning ability. Our investigation shows the potential of DepictQA to integrate individual preferences into the evaluation process. We also demonstrate the utility of our full-reference

dataset in non-reference applications. These results attest to the superiority of DepictQA, and the research potential of Multi-modal IQA tasks.

2 Related Works

Score-based IQA methods. Most existing IQA methods rely on scores to assess image quality. They can be categorized into *full-reference* and *non-reference* methods. (1) Full-reference methods assess image quality by computing the similarity score between a distorted image and a high-quality reference image. Traditional methods rely on human-designed metrics like structural similarity [55], image information [46], phase congruency with gradient magnitude [62], *etc.* Learning-based methods aim to align with human assessment through data-driven training. LPIPS [64] shows that the learned features can effectively function as a perceptual metric, exhibiting high consistency with human judgments. In alignment with advancements in the deep-learning community, data-driven approaches [4, 6, 10, 11, 13, 43, 60, 69] have similarly spurred innovations in IQA. (2) Non-reference methods evaluate the quality of a distorted image without a reference image. Traditional methods [30–35, 45, 50] primarily calculate quality scores based on human-designed natural image statistics. Deep-learning-based methods [20, 21, 29, 39, 47, 68, 71] replace hand-crafted statistics by learning quality priors from extensive data. Recent works further enhance the performance by introducing graph representation [48], CLIP pre-training [54], continual learning [65], multitask learning [66], and so on. However, score-based IQA methods exhibit inherent limitations, particularly the inability to reflect the intricate analyses and weights of multiple aspects, as discussed in Sec. 1.

Multi-modal Large Language Models (MLLMs) incorporate other modalities (especially visions) into LLMs by leveraging the emergent ability of LLMs [36]. Early efforts [7, 53] primarily focus on data-efficient fine-tuning, while recent advancements [12, 18] build end-to-end trainable frameworks on web-scale multi-modal corpora. Various approaches choose to train different modules, *e.g.*, the vision-to-text alignment modules [25, 70], the medium-gated layers [1], and the core LLMs [28, 59]. Recent studies emphasize integrating the intermediate features [14, 24, 63], improving in-context learning [67], and establishing comprehensive multi-modal benchmarks [61], *etc.* Recently, GPT-4V [37] has showcased remarkable capabilities in general visual understanding. However, we demonstrate in Sec. 5.3 that general MLLMs are not good at IQA tasks.

MLLMs for IQA. Recently, Q-Bench [56] constructs a comprehensive benchmark to assess existing MLLMs in low-level perception tasks. Q-Instruct [57] further promotes the low-level perception ability of MLLMs by introducing a large-scale dataset. Q-Align [58] takes advantage of the text-guided instruction tuning for more accurate quality score regression. Our work distinguishes itself from existing works. Our focus lies on quality comparison regarding distortions and texture damages across multiple images, whereas existing works primarily center on low-level perception and score regression within individual images.

(a) Task—1: Quality Description

Texture Category: Water Surface, Fabrics, **Plants, Foliage**, Faces,

Texture Condition: Clearly identifiable, Barely identifiable, Completely damaged

Distortion: Brightness Distortion: Undistorted, Mild, Severe; Color Distortion: Undistorted, Mild, Severe; Noise: Undistorted, Mild, Severe; Artifacts: Undistorted, Mild, Severe; Blurriness: Undistorted, Mild, Severe

Overall Quality: Distorted Image is: Nearly undistorted, Mild distortion, Severe distortion

Generate Structured Quality Descriptions with GPT-4

Annotations: **Revised Generated Texts**

Response for Quality Description: The overall quality of this image has been severely compromised, particularly in color distortion and noise, resulting in a significant deviation in the overall visual perception of the image, despite maintaining good consistency in terms of brightness, artifacts, and blurring. In terms of texture quality, the plant textures are barely recognizable, primarily due to the influence of color distortion and noise. Therefore, the severe distortion in color and noise has significantly affected the overall and texture quality of the image.

(b) Task—2: Quality Comparison

Human-Annotated Two-Alternative Forced Choice Result: **A > B**, A < B

Sample from GPT-4 Generated One-Sentence Comparative Conclusion

Response for Quality Comparison: Image A maintains a distinct advantage in terms of image quality over Image B, substantiating its superior qualities.

(c) Task—3: Comparison Reasoning

Texture Category: Plants, Foliage, **Faces**,

Texture of Image A: Clearly identifiable, Barely identifiable, Completely damaged

Texture of Image B: Clearly identifiable, Barely identifiable, Completely damaged

Distortion: Brightness Distortion: A << B, **A < B**, A = B, A > B, A >> B; Color Distortion: A << B, A < B, **A = B**, A > B, A >> B; Noise: A << B, A < B, **A = B**, A > B, A >> B; Artifacts: A << B, A < B, **A = B**, A > B, A >> B; Blurriness: A << B, A < B, A = B, A > B, **A >> B**

Overall Comparison: Comparison result is: A is better than B, A is slightly better, A is worse than B, A is slightly worse, Hard to decide

Generate Structured Quality Descriptions with GPT-4

Annotations: **Revised Generated Texts**

Response for Comparison Reasoning: Although Image A is slightly inferior to Image B in terms of brightness distortion, it significantly outperforms Image B. From the perspective of overall distortion, Image A far outperforms Image B. Image A can clearly identify the facial textures, whereas the facial textures in Image B are completely damaged and unidentifiable. Therefore, despite Image A's slight inferiority in brightness distortion, its advantages in blurriness and its ability to clearly identify textures, result in Image A's overall quality being superior.

Fig. 2: Collection of the responses in our M-BAPPS dataset. We first carefully design a questionnaire to collect quality-related information. We then employ the GPT-4 [36] to convert our annotated questionnaire results into natural language. Finally, the outputs of GPT-4 are modified and improved by the annotators to correct errors, eliminate ambiguities, and supplement important information.

3 DepictQA Task and Dataset

3.1 Task Description

Before introducing our method, we need to rethink the paradigm of IQA. To reflect the human process of assessing image quality, we intend to apply language as a powerful interactive tool. Intuitively, DepictQA needs the following abilities.

First, DepictQA needs to **identify the distortions and texture damages** (Fig. 2a). Humans begin assessing image quality by identifying distortions and texture damages, as this is the basis for any subsequent assessment.

Second, DepictQA is required to **compare distorted images** like Fig. 2b rather than just calculate scores for individual images. Quantifying image quality has drawbacks, as the information from a single score is quite limited. It has also been verified that humans tend to make a biased quality assessment on a single image, but are more consistent and reliable in comparing two images [15, 16, 40].

Third, DepictQA should **weigh and judge multiple aspects** that affect image quality. Humans consider many factors when comparing image quality. For example, when comparing an underexposed image and a blurry image in Fig. 2c, one may need to consider the real impacts of these two distortions on the texture representation, and weigh among these considerations. DepictQA should mimic this weighing ability, which distinguishes it from previous IQA methods.

Based on the above discussion, as described in Fig. 2, we design a hierarchical task paradigm, progressively guiding DepictQA to obtain the above abilities:

- *Task-1: Quality Description.* Based on the provided reference image and a distorted image, describe the distortions and texture damages in the distorted image, and comment on the overall quality of the distorted image.
- *Task-2: Quality Comparison.* Based on the provided reference image and its two distorted versions, determine which distorted image has a better quality.
- *Task-3: Comparison Reasoning.* Based on the comparison result, describe the distortions and texture damages of the two distorted images, make inferences, and weigh the pros and cons to justify its judgment on image quality.

3.2 Dataset Construction

Data serves as the key factor for training MLLMs. We follow the scheme of supervised fine-tuning [28,61] to train DepictQA. Supervised fine-tuning requires collecting {images, question, response} data pairs, where “images” are the ones to be evaluated, “question” describes the task, and “response” is the reference answer. In this section, we describe in detail our selection of images and the collection of questions and responses for the three tasks.

Image collection for the IQA dataset consists of two aspects, one is the selection of reference images, and the other is the collection of distorted images. Existing works usually collect a large number of distorted images on a small number of reference images [15,16,40,43]. However, the semantic richness of the training images is also very important. In our work, we collect reference images and their corresponding distorted images from the BAPPS dataset [64]. BAPPS dataset contains 197k highly diverse samples, meeting the diversity requirements of DepictQA training. For each sample, there is a reference image and its two distorted versions, as given in Fig. 2b and 2c. BAPPS dataset also provides human annotations, indicating which distorted image is more similar to the reference one, *i.e.*, has better perceptual quality. These annotations can be used to build our dataset and validate our newly annotated data.

Question collection. For each task, users may express similar questions in different sentences, like the two questions in Fig. 1. To encourage the robustness of DepictQA to users’ questions, for each task, we first leverage GPT-4 to generate 30 questions. We then manually remove ambiguous and duplicate questions and modify inaccurate questions to form a set of 10 questions (see *Appendix*). During training and testing, we randomly sample a question from the question set to construct the data pair.

Response collection. A straightforward way to collect high-quality training texts is manually writing [38,52]. However, when annotators are inexperienced or tired, human-written texts can lead to biases and uneven quality. In this work, we use advanced LLMs to assist annotators in generating structured training texts, as shown in Fig. 2. We first collect the information that we want the texts to describe through a carefully designed questionnaire. Answering questions greatly reduces the possibility of ambiguity among annotators and ensures that

the information is structured. We then use GPT-4 to convert our annotated questionnaire results into natural language. Finally, the outputs of GPT-4 are modified and improved by the annotators to correct errors, eliminate ambiguities, and add important information. This process greatly reduces the difficulty of collecting training texts and improves the quality of the training texts. Next, we introduce the details of the questionnaire for different tasks.

Task-1: Quality Description. A distorted image and its reference image are shown to annotators. Fig. 2a shows our questionnaire with three parts: texture, distortion, and overall quality. For the texture part, annotators are asked to select the one that best matches the image from a list containing 11 typical texture types, including object edges, bricks, fabrics, plants or foliage, architectures, artificial strips, hairs or furs, faces, sky or clouds, stones or ground, and water surface. These 11 types are selected based on the existing IQA [16] and texture recognition [2] research. Additionally, annotators are asked to indicate whether the texture is “clearly identifiable”, “barely identifiable”, or “completely damaged”. Regarding the distortion part, we ask annotators to summarize with the following five aspects: “brightness”, “color”, “noise”, “artifacts”, and “blurriness”. For each distortion, we use three levels for evaluation: “undistorted”, “mild”, and “severe”. This can express most distortions that appear in images. Finally, annotators need to comment on the overall quality of the image into three levels: “nearly undistorted”, “mild distortion”, and “severe distortion”.

Task-2: Quality Comparison. BAPPS dataset already includes binary comparison labels (*i.e.*, Image A or Image B is better) for all image pairs. To convert these comparison labels into textural responses, we first build a response pool using GPT-4, including 20 generated sentences for “Image A is better” and another 20 for “Image B is better”. Then, for each comparison label, we randomly sample one response from the pool, as depicted in Fig. 2b. However, the diversity of language output poses a challenge to evaluation. For the convenience of evaluation, inspired by LLaVA-1.5 [27], we randomly sample half of the questions and add the following short answer prompt: “Answer the question using a single word or phrase”. Correspondingly, the response will be a single phrase like “Image A” or “Image B” indicating the less distorted image.

Task-3: Comparison Reasoning. As shown in Fig. 2c, annotators are given two distorted images and the reference image. The annotation pipeline is similar to Task-1. Annotators compare two distorted images from the five kinds of distortions and the overall distortion using five options: “superior” ($>>$), “slightly superior” ($>$), “roughly equal” (\approx), “slightly inferior” ($<$), and “inferior” ($<<$).

Dataset statistics. The statistics of our dataset are presented in Tab. 1 (more in *Appendix*). Our dataset comprises 5,104 detailed high-quality samples (Task-1 and Task-3), along with 115,646 brief templated samples (training set of Task-2). The validation set of Task-2 is the same as the “Traditional” and “CNN”

Table 1: Statistics of M-BAPPS dataset.

	# Task-1 Quality Description	# Task-2 Quality Comparison	# Task-3 Comparison Reasoning
Train	1,115	115,646	3,739
Validation	50	9,440	200
Total	1,165	125,086	3,939

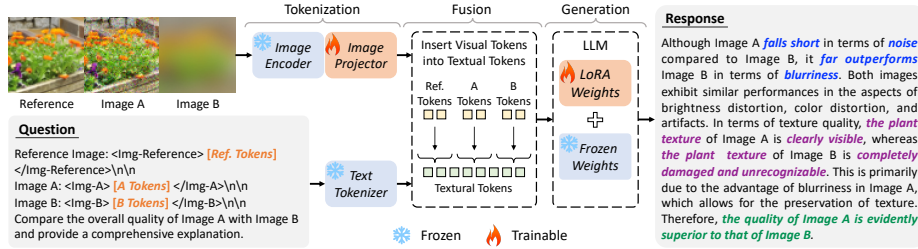


Fig. 3: Framework of DepictQA. A frozen pre-trained image encoder is employed to encode images to visual tokens, followed by a trainable image projector to project visual tokens to textual space. The question texts are tokenized by a text tokenizer. Visual tokens and textual tokens are then fused and jointly processed by an LLM, fine-tuned through the LoRA technique [17]. Our model is capable of producing comprehensive and informative explanations for image quality comparisons.

categories (two sets of distortions) in BAPPS’s validation set [64]. Each training sample is individually annotated by one annotator. In the validation set, samples are annotated by two annotators only if they reach a consensus. As a means of verification, the annotated “Overall Comparison” judgments in Task-3 exhibit a quite high consistency rate of 84.3% with the ground-truth judgments in the BAPPS dataset. For brevity, the three tasks will be shortened to *description*, *comparison*, and *reasoning* in the following.

4 DepictQA Framework

4.1 Model Architecture

Fig. 3 shows the workflow of our DepictQA. DepictQA takes images and a quality-related question as inputs, and generates a descriptive text as the response. In *comparison* or *reasoning* tasks, there are three input images: a reference image and Image A and B. In *description* task, there are two input images: a reference image and a distorted image. The input images and the question are first tokenized, then fused, finally processed by the LLM for response generation.

Tokenizing input images and question. As shown in Fig. 3, we employ a frozen CLIP pre-trained ViT-L/14 [44] as the image encoder to represent the input images as visual tokens. Then, the question texts are tokenized to textual tokens by SentencePiece tokenizer [22]. The visual tokens cannot be directly processed by the LLM due to different embedding spaces, so we use a trainable image projector to map visual tokens into the textual space as in [28, 70].

Token fusion. We insert the visual tokens into pre-defined positions within the textual tokens for token fusion, *i.e.*, [Ref. Tokens], [A Tokens], [B Tokens] in the input question in Fig. 3.

Response generation using LLM. The fused tokens are fed into LLM to generate the final response. Our DepictQA is compatible with different LLMs (Vicuna-v0-7B [8], Vicuna-v1.5-7B [8], and LLaMA-2-chat-7B [52]), as shown in

Tab. 5. Pre-trained LLMs do not work well on IQA tasks, and need to be fine-tuned on our dataset. However, complete LLM fine-tuning is resource-intensive and data-hungry, requiring tens of thousands of high-quality human-written texts [38]. To get around of data shortage issue, we resort to LoRA [17], an efficient LLM fine-tuning technique, which selectively adjusts only a small set of parameters in the LLM. Following [17, 61], we apply LoRA to fine-tune the projection layers in all self-attention modules.

Unique tag to distinguish multiple images. Existing MLLMs [28, 70] are primarily designed to handle a single input image. They insert the visual tokens between the start (*e.g.*, ``) and end (*e.g.*, ``) tags. A simple extension to multi-image input is using textual cues to distinguish images, *e.g.*, adding “Reference Image:”, “Image A:”, and “Image B:” before visual tokens. However, this simple extension sometimes fails to distinguish images, probably because the proportion of these short textual cues in the full texts is too small. To mitigate this, motivated by [67], we adopt the unique tag for each image. In *comparison* and *reasoning* tasks, we select `<Img-Reference>`, `<Img-A>`, and `<Img-B>` as start tags, adhering to the HTML rule by adding a trailing slash (“/”) in the end tags. In *description* task, the reference image retains the same tags, while the distorted image employs the original tags, ``.

4.2 Training Scheme

Multi-source training data. As stated in Sec. 1, our training images come from three sets: (1) 115,646 brief templated data of Task-2 (*comparison*), (2) 4,854 high-quality data of Task-1 (*description*) and Task-3 (*reasoning*), which are duplicated by 20 times to increase the training weights, and (3) 48,734 content description data (Detailed Description dataset in [61], duplicated 2 times during training), which are unrelated to IQA. The abundant templated data principally bridge images and descriptive texts in quality-related tasks. The limited yet high-quality data foster the model’s descriptive and reasoning skills. The IQA-unrelated content description data can serve as regularization, given the limited text diversity of our IQA data for an MLLM. Experimental results in Tab. 4 prove the effectiveness of the three sources of training data.

Training objective. Following existing works [5, 28, 61], the training objective of DepictQA is the next token prediction loss: a cross-entropy loss between predicted and ground-truth next tokens. Only the tokens in the responses contribute to the loss computation. Also, only the image projection layer and LoRA parameters are optimized, comprising a mere 0.25% of the total parameters.

5 Experiments

This section discusses experimental setups and results. In our experiments, we set the LoRA rank to 16. The image size in BAPPS dataset [64] is 64×64 , and we zero-pad it to 70×70 , then encode it into 25 tokens. DepictQA is trained for 1 epoch with batch size 64. Adam optimizer with $(\beta_1, \beta_2) = (0.9, 0.95)$, weight decay 0.001, and learning rate 0.0005 is used for training.

5.1 Metrics

Unlike traditional score-based IQA methods, evaluating the diverse, descriptive, and textual results of multi-modal IQA methods is not trivial. Therefore, we adopt three different metrics for a comprehensive evaluation.

Accuracy. For *comparison* task, we employ the accuracy metric. MLLMs usually produce diverse textual outputs, necessitating transformation to bi-classification results (*i.e.*, Image A or Image B is better) for accuracy calculation. As described in the *Task-2* part in Sec. 3.2, we add the short answer prompt “Answer the question using a single word or phrase” during training, guiding DepictQA to directly output bi-classification results.

GPT4-score. For *description* and *reasoning* tasks, following [8,28], we utilize the GPT4-score for assessment. Specifically, we provide GPT-4 with all information in the human-labeled questionnaire as context. Then, we give GPT-4 both the model-generated response and the corresponding ground truth response. Based on the context, GPT-4 evaluates the helpfulness, relevance, accuracy, and level of detail of these two responses, and gives an overall score on a scale of 0 to 10, where a higher score indicates better quality. Finally, the relative score with regard to the ground truth response is reported as the GPT4-score.

Reasonable rate by human evaluators. We observe that the GPT4-score exhibits excessive confidence in some low-quality responses. In some cases, a fully wrong response even receives a GPT4-score over 60% (see *Appendix*). Consequently, for a more comprehensive evaluation, given both the images and responses, human evaluators label each response as reasonable or unreasonable. A reasonable response should adhere to three criteria: indicating major distortions, no severe mistakes, and logical self-consistency, which are detailed in *Appendix*. The reasonable rate also serves as another metric to assess description and reasoning ability.

5.2 Comparison with Score-based IQA Methods

To demonstrate the effectiveness of DepictQA, we compare it with score-based IQA methods on the *comparison* task (Task-2). We evaluate four traditional IQA methods including PSNR, SSIM [55], VIF [46], and FSIM [62], and four deep-learning-based IQA methods including DeepIQA [3], PieAPP [43], LPIPS [64], and DISTS [11]. Here our base LLM is selected as LLaMA-2-chat-7B [52].

Quantitative results of quality comparison on BAPPS are depicted in Tab. 2a. Our DepictQA surpasses the best traditional method, FSIM, by a large margin ($\sim 11\%$). We also stably outperform the best deep-learning-based competitors, LPIPS and DISTS ($>2.6\%$), even near the human performance. We show in Tab. 5 that the accuracy could be further enhanced with pre-training initialization (but with near $3\times$ training time). Unlike high-level perception tasks where multi-modal approaches usually lag behind single-modal methods [61], we show that multi-modal IQA methods can surpass score-based counterparts in the quality comparison task. Nevertheless, the quantitative comparison is not the key issue, we pay more attention to the description and reasoning abilities.

Table 2: Quantitative results of quality comparison task with accuracy metric. Our DepictQA achieves the state-of-the-art performance.

(a) Evaluation on BAPPS benchmark [64].					(b) Evaluation on benchmark datasets including LIVE-MD [19], MDID2013 [49], CSIQ [23], TID2013 [41], KADID [26], and PIPAL [16].			
Type	Method	Distortion	Category	Average	Datasets	Methods		
		Traditional	CNN			PieAPP [43]	LPIPS [64]	DepictQA (Ours)
Oracle	Human	80.8	84.4	82.6	LIVE-MD	83.6	91.1	95.4
Traditional	PSNR	59.9	77.8	68.9	MDID2013	83.7	88.1	91.3
	SSIM [55]	60.3	79.1	69.7	CSIQ	84.9	87.3	87.9
	VIF [46]	55.6	74.4	65.0	TID2013	77.2	86.6	89.6
	FSIM [62]	62.7	79.4	71.0	KADID	70.1	79.8	91.5
Learning	DeepIQA [3]	70.3	79.4	74.8	PIPAL	66.3	84.8	86.5
	PieAPP [43]	72.7	77.0	74.6				
	LPIPS [64]	76.0	<u>82.8</u>	79.4				
	DISTS [11]	<u>77.2</u>	82.2	<u>79.7</u>				
DepictQA (Ours)		80.3	84.2	82.3				

Quantitative results of quality comparison on multiple IQA datasets are shown in Tab. 2b. We include additional experiments for the *comparison* task on the following IQA datasets: LIVE-MD [19], MDID2013 [49], CSIQ [23], TID2013 [41], KADID [26], and PIPAL [16]. These datasets consist of reference images and corresponding distorted versions. To adapt them to the quality comparison task, we reorganize the datasets by randomly selecting a reference image and its two distortions. The ground truth is established by comparing the MOS or DMOS of these two distorted images. The classification accuracy is reported as the metric. The results show that our DepictQA outperforms two baselines on all datasets, validating its effectiveness across multiple datasets.

5.3 Comparison with General Multi-modal LLMs

We further compare DepictQA with general Multi-modal LLMs (MLLMs) on the validation sets of *description* (Task-1) and *reasoning* (Task-3) tasks. We also transform the reasoning responses to bi-classification results to calculate the comparison accuracy. We choose three MLLMs as baselines: LLaVA [28], LLaVA-1.5 [27], MiniGPT4 [70], and LAMM [61]. The model weights are obtained from their official GitHub repositories. We provide explicit and comprehensive task instructions to inform the MLLMs of the task definition.

Quantitative results are illustrated in Tab. 3. LLaVA and MiniGPT4 (LLaMA-2-chat) fail in IQA tasks, yielding either nearly identical results or irrelevant results across most samples. Other general MLLMs exhibit poor performance, indicating their inadequacy for IQA tasks. However, after fine-tuning on our M-BAPPS dataset, DepictQA achieves significantly improved performance.

Qualitative results. Three qualitative results of *reasoning* task are depicted in Fig. 1 and Fig. 3. More qualitative results and failure cases of *description*, *comparison*, and *reasoning* tasks are illustrated in *Appendix*.

Table 3: Performance comparison of DepictQA and general MLLMs. All LLMs have 7B parameters, and “LLaMA-2c” means “LLaMA-2-chat”. The comparison ability is evaluated by accuracy. Since general MLLMs can produce responses without explicit comparison results, accuracy is reported with these responses included / excluded. The description and reasoning abilities are assessed using the reasonable rate / GPT4-score. Obviously, general MLLMs are not capable of IQA tasks.

Method	LLaVA [28]	LLaVA-1.5 [27]	MiniGPT4 [70]	MiniGPT4 [70]	LAMM [61]	LAMM [61]	DepictQA (Ours)
LLM (7B)	LLaMA-2c	Vicuna-v1.5	Vicuna-v0	LLaMA-2c	Vicuna-v0	LLaMA-2c	Vicuna-v1.5
Description	fail	18.0 / 65.8	16.0 / 49.9	fail	12.0 / 62.5	8.0 / 57.4	64.0 / 76.2
Comparison	fail	43.0 / 50.6	38.0 / 46.3	fail	53.0 / 55.8	44.0 / 48.9	82.0
Reasoning	fail	7.0 / 63.9	1.0 / 42.4	fail	4.0 / 58.1	5.0 / 52.4	53.0 / 76.4

5.4 Ablation Studies

We conduct extensive ablation studies to verify the effectiveness of our methodologies. The LLM used in ablation studies is Vicuna-v1.5-7B [8] if not specified.

Effects of multi-source training data are detailed in Tab. 4. (1) Task-2 data (*comparison*) remarkably improves comparison accuracy (#2 *vs.* #4). Even though these texts are brief and templated, the abundant samples still help bridge the images and texts in quality-related tasks. (2) As evidenced by #1 *vs.* #4 and #3 *vs.* #5, Task-3 data (*reasoning*) is necessary for a robust reasoning ability. Task-1 data (*description*) boosts reasoning metric (#4 *vs.* #5), mainly by helping identify distortions. Therefore, the high-quality texts of Task-1 and Task-3 are necessary for DepictQA to depict the image quality with language. (3) However, as shown by #1 *vs.* #3 and #4 *vs.* #5, Task-1 data (*description*) harms the comparison performance because of the gap between the two tasks in prompts and the number of input images. (4) Fortunately, the harms can be eliminated by integrating content description data (#5 *vs.* #6), which serves as regularization in light of M-BAPPS’s limited text variety for an MLLM. Additionally, the content description data also helps enrich the text diversity, as shown in *Appendix*.

Unique tag effectively mitigates the confusion problem, detailed in Fig. 4. Confusion occurs when distortions in one image are mistakenly attributed to another. To quantify this, we manually review 50 responses and compute the confusion rate. With the unified tag, the model needs to distinguish images through textual hints, as stated in Sec. 4.1, leading to a 24% confusion rate. One unique tag for each image significantly reduces the confusion rate to 12%.

The size of training data is studied in Fig. 5. As the size of training data increases, the comparison performance gradually increases. Thus the quantity of the training data still plays a key role in the MLLM-based method.

LLMs and the initialization methods are studied in Tab. 5. For random initialization, we retrain the image projector and LoRA parameters from scratch. For high-level initialization, trainable parameters are pre-trained on high-level perception tasks (*e.g.*, description and caption). (1) Overall, our DepictQA is compatible with different LLMs, stably yielding high performance. Also, the performance is slightly improved with more advanced LLMs (*e.g.*, Vicuna-v1.5

Table 4: Ablation studies of multi-source training data. “Cont.” means the content description data. The comparison ability is assessed by accuracy within Traditional / CNN categories. The reasoning ability is evaluated by reasonable rate / GPT4-score. Training with multi-source data stably improves the performance.

#	Training Data				Comparison Reasoning	
	Task2	Task1	Task3	Cont.		
1	✓				78.6/82.5	N/A
2			✓		66.4/65.4	31.0/74.2
3	✓	✓			76.3/80.5	N/A
4	✓		✓		79.7/83.3	41.0/74.3
5	✓	✓	✓		78.1/82.9	45.0/ 77.2
6	✓	✓	✓	✓	80.0/83.8	53.0/76.4

	Unified Tag: for all three images Response: ...Image A <i>underperforms</i> Image B in terms of <i>color distortion</i> . However, Image A <i>excels in noise control</i> , clearly outperforming Image B...	
	Unique Tag: <img-Reference>, <img-A>, <img-B> Response: ...Although Image A <i>slightly outperforms</i> in terms of <i>color distortion</i> , it is markedly <i>inferior to</i> Image B in the aspect of <i>noise</i> ...	
		
	Unified Tag	Unique Tag
Confusion Rate / %	24.0	12.0

Fig. 4: Unique tag alleviates the confusion problem using clearer instructions. The confusion rate drops dramatically.

Table 5: Ablation studies of LLMs and initialization methods. “High-level” means the MLLM is pre-trained on high-level perception tasks. The comparison ability is evaluated by accuracy within Traditional / CNN categories. DepictQA is compatible with different LLMs. Pre-training on high-level perceptual tasks improves the performance.

#	LLM	Init.	Comparison
1	Vicuna-v0-7B	Random	79.5/83.7
2	Vicuna-v0-7B	High-level	79.8/84.2
3	Vicuna-v1.5-7B	Random	80.0/83.8
4	Vicuna-v1.5-7B	High-level	81.2/85.3
5	LLaMA-2-chat-7B	Random	80.3/84.2
6	LLaMA-2-chat-7B	High-level	80.1/ 85.1

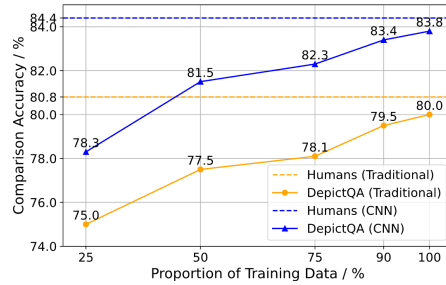


Fig. 5: The comparison performance gradually increases with the size of training data increasing.

and LLaMA-2-chat). (2) With the same LLM, pre-training on high-level perceptual tasks further enhances the overall performance. Nevertheless, pre-training will also increase the training time by nearly three times.

5.5 Comparison with GPT-4V

We compare DepictQA with GPT-4V [37] on the first 100 samples in the validation set of Task-3 (*reasoning*). We request GPT-4V to complete both *comparison* and *reasoning* tasks. GPT-4V is given detailed instructions and two human-labeled examples for task description. As shown in Tab. 6, our DepictQA and GPT-4V have mutual advantages and disadvantages. The GPT4-score of GPT-4V is quite high, even higher than human-annotated responses (>100%), because of the linguistic fluency and detailed description of

Table 6: Comparison with GPT-4V [37]. The comparison ability is assessed by accuracy, while the reasoning ability is evaluated by reasonable rate / GPT4-score.

Method	Comparison	Reasoning
GPT-4V [37]	65.0	52.0 / 106.4
DepictQA (ours)	90.0	53.0 / 77.6

image contents. However, we achieve comparable performance at the human-evaluated reasonable rate. Moreover, the quality comparison ability of DepictQA is significantly better than GPT-4V. Note that GPT-4V is close-source and expensive to access, thus developing an effective MLLM for IQA is worthwhile. See *Appendix* for qualitative results and failure cases of GPT-4V.

5.6 Complexity and Efficiency

Training cost. The trainable parameters in DepictQA are 16M, constituting only 0.25% of the total parameters (7B). DepictQA is trained on 8 GPUs (NVIDIA RTX A6000 48G). The training is completed in around 6 hours.

Inference cost. The inference time depends on the response length and is tested on a single A6000 GPU on the BAPPS dataset [64]. (1) For *comparison* task with short answer prompt (2 words), the inference time stands at approximately 2.20s / batch=32, transformed to 0.07s / sample. (2) For *comparison* task without short answer prompt (~ 10 words), the inference time is 2.76s / batch=32 (*i.e.*, 0.09s / sample) on average. (3) Regarding *reasoning* task (~ 143 words), the inference time is around 20.86s / batch=32 (*i.e.*, 0.65s / sample). Despite the incorporation of MLLMs that are known to be resource-intensive, our DepictQA remains deployable on a single consumer GPU (*e.g.*, RTX3090).

6 Extensions and Limitations

Table 7: Comparison performance in the non-reference scenarios on BAPPS benchmark [64]. The comparison ability is evaluated by accuracy within Traditional / CNN categories.

Training data	Comparison
Full-reference	67.5 / 69.5
Full-reference & Non-reference	76.7 / 80.2

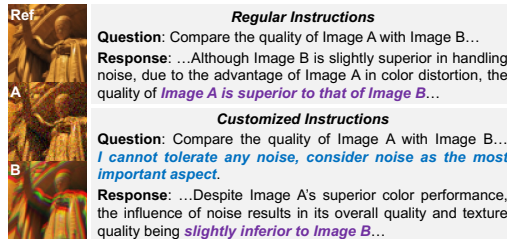


Fig. 6: DepictQA has the potential to be a customized IQA tool by incorporating human preferences into instructions.

Non-reference applications. Although our dataset is initially gathered in a full-reference setting, we demonstrate its utility in non-reference applications. Here we select *comparison* task in the non-reference setting on BAPPS benchmark [64], *i.e.*, directly compare the quality of two distorted images without the reference image. As indicated in Tab. 7, training solely on full-reference data leads to subpar performance. We thus generate non-reference training data by removing the reference image in our original dataset. Incorporating this non-reference data notably improves the model’s non-reference comparison abilities.

Potential to be customized. Given various instructions, DepictQA has the potential to be a customized IQA tool. To demonstrate this potential, as shown in Fig. 6, we append the specific human preference (*e.g.*, cannot tolerate any

noise) to the instructions, DepictQA adapts its comparison results accordingly. How to better induce this ability is our future work.

Limitations. In this preliminary attempt, we demonstrate the possibility of depicting image quality with MLLMs. There is still a long way to go for real-world application. (1) The amount and coverage of data are not sufficient, limiting the generalization to real-world images. (2) The performance in *description* and *reasoning* tasks is not satisfying, particularly in the human-evaluated reasonable rate. (3) The distortion types can be more than five, even not pre-defined. Also, more fine-grained comparisons focusing on local details are preferred. (4) Finally, whether MLLM-based IQA methods can take the place of score-based ones is still an open question. These belong to our future works.

7 Conclusion

We propose DepictQA, employing MLLMs for descriptive and human-like IQA. DepictQA differs from traditional score-based methods by describing and comparing image distortions and texture damages with languages, well aligned with the humans' evaluation process. For DepictQA development, we create a hierarchical task paradigm and gather a multi-modal IQA dataset. DepictQA surpasses score-based method in multiple IQA benchmarks and outputs more precise description and reasoning results than general MLLMs. Our work also reveals the adaptability of language-based IQA methods for individual preferences.

References

1. Alayrac, J.B., Donahue, J., Luc, P., Miech, A., Barr, I., Hasson, Y., Lenc, K., Mensch, A., Millican, K., Reynolds, M., et al.: Flamingo: a visual language model for few-shot learning. In: NeurIPS (2022) 4
2. Bell, S., Upchurch, P., Snavely, N., Bala, K.: Material recognition in the wild with the materials in context database. In: CVPR (2015) 7
3. Bosse, S., Maniry, D., Müller, K.R., Wiegand, T., Samek, W.: Deep neural networks for no-reference and full-reference image quality assessment. IEEE TIP (2017) 10, 11
4. Bosse, S., Maniry, D., Müller, K.R., Wiegand, T., Samek, W.: Deep neural networks for no-reference and full-reference image quality assessment. IEEE TIP (2018) 4
5. Brown, T., Mann, B., Ryder, N., Subbiah, M., Kaplan, J.D., Dhariwal, P., Neelakantan, A., Shyam, P., Sastry, G., Askell, A., et al.: Language models are few-shot learners. In: NeurIPS (2020) 9
6. Cao, Y., Wan, Z., Ren, D., Yan, Z., Zuo, W.: Incorporating semi-supervised and positive-unlabeled learning for boosting full reference image quality assessment. In: CVPR (2022) 4
7. Chen, J., Guo, H., Yi, K., Li, B., Elhoseiny, M.: Visualgpt: Data-efficient adaptation of pretrained language models for image captioning. In: CVPR (2022) 4
8. Chiang, W.L., Li, Z., Lin, Z., Sheng, Y., Wu, Z., Zhang, H., Zheng, L., Zhuang, S., Zhuang, Y., Gonzalez, J.E., et al.: Vicuna: An open-source chatbot impressing gpt-4 with 90%* chatgpt quality. <https://vicuna.lmsys.org> (2023) 8, 10, 12, 20, 22

9. Devlin, J., Chang, M.W., Lee, K., Toutanova, K.: Bert: Pre-training of deep bidirectional transformers for language understanding. arXiv preprint arXiv:1810.04805 (2018) [21](#)
10. Ding, K., Liu, Y., Zou, X., Wang, S., Ma, K.: Locally adaptive structure and texture similarity for image quality assessment. In: ACM MM (2021) [4](#)
11. Ding, K., Ma, K., Wang, S., Simoncelli, E.P.: Image quality assessment: Unifying structure and texture similarity. IEEE TPAMI (2020) [4](#), [10](#), [11](#)
12. Driess, D., Xia, F., Sajjadi, M.S., Lynch, C., Chowdhery, A., Ichter, B., Wahid, A., Tompson, J., Vuong, Q., Yu, T., et al.: Palm-e: An embodied multimodal language model. arXiv preprint arXiv:2303.03378 (2023) [4](#)
13. Ghildyal, A., Liu, F.: Shift-tolerant perceptual similarity metric. In: ECCV (2022) [4](#)
14. Gong, T., Lyu, C., Zhang, S., Wang, Y., Zheng, M., Zhao, Q., Liu, K., Zhang, W., Luo, P., Chen, K.: Multimodal-gpt: A vision and language model for dialogue with humans. arXiv preprint arXiv:2305.04790 (2023) [4](#)
15. Gu, J., Cai, H., Chen, H., Ye, X., Ren, J., Dong, C.: Image quality assessment for perceptual image restoration: A new dataset, benchmark and metric. arXiv preprint arXiv:2011.15002 (2020) [1](#), [5](#), [6](#)
16. Gu, J., Cai, H., Chen, H., Ye, X., Ren, J., Dong, C.: Pipal: a large-scale image quality assessment dataset for perceptual image restoration. arXiv preprint arXiv:2007.12142 (2020) [5](#), [6](#), [7](#), [11](#)
17. Hu, E.J., Wallis, P., Allen-Zhu, Z., Li, Y., Wang, S., Wang, L., Chen, W., et al.: Lora: Low-rank adaptation of large language models. In: ICLR (2021) [8](#), [9](#)
18. Huang, S., Dong, L., Wang, W., Hao, Y., Singhal, S., Ma, S., Lv, T., Cui, L., Mohammed, O.K., Liu, Q., et al.: Language is not all you need: Aligning perception with language models. arXiv preprint arXiv:2302.14045 (2023) [3](#), [4](#)
19. Jayaraman, D., Mittal, A., Moorthy, A.K., Bovik, A.C.: Objective quality assessment of multiply distorted images. In: Conference record of the forty sixth Asilomar conference on signals, systems and computers (ASILOMAR) (2012) [11](#)
20. Kang, L., Ye, P., Li, Y., Doermann, D.: Convolutional neural networks for no-reference image quality assessment. In: CVPR (2014) [4](#)
21. Ke, J., Wang, Q., Wang, Y., Milanfar, P., Yang, F.: Musiq: Multi-scale image quality transformer. In: CVPR (2021) [4](#)
22. Kudo, T., Richardson, J.: Sentencepiece: A simple and language independent subword tokenizer and detokenizer for neural text processing. In: Proceedings of the 2018 Conference on Empirical Methods in Natural Language Processing: System Demonstrations (2018) [8](#)
23. Larson, E.C., Chandler, D.M.: Most apparent distortion: full-reference image quality assessment and the role of strategy. Journal of electronic imaging (2010) [11](#)
24. Li, B., Zhang, Y., Chen, L., Wang, J., Yang, J., Liu, Z.: Otter: A multi-modal model with in-context instruction tuning. arXiv preprint arXiv:2305.03726 (2023) [4](#)
25. Li, J., Li, D., Savarese, S., Hoi, S.: Blip-2: Bootstrapping language-image pre-training with frozen image encoders and large language models. arXiv preprint arXiv:2301.12597 (2023) [4](#)
26. Lin, H., Hosu, V., Saupe, D.: Kadid-10k: A large-scale artificially distorted iqa database. In: Eleventh International Conference on Quality of Multimedia Experience (QoMEX) (2019) [11](#)
27. Liu, H., Li, C., Li, Y., Lee, Y.J.: Improved baselines with visual instruction tuning. arXiv preprint arXiv:2310.03744 (2023) [7](#), [11](#), [12](#)

28. Liu, H., Li, C., Wu, Q., Lee, Y.J.: Visual instruction tuning. arXiv preprint arXiv:2304.08485 (2023) [2](#), [3](#), [4](#), [6](#), [8](#), [9](#), [10](#), [11](#), [12](#), [22](#)
29. Liu, X., van de Weijer, J., Bagdanov, A.D.: RankIQA: Learning from rankings for no-reference image quality assessment. In: ICCV (2017) [4](#)
30. Ma, C., Yang, C.Y., Yang, X., Yang, M.H.: Learning a no-reference quality metric for single-image super-resolution. Computer Vision and Image Understanding (2017) [4](#)
31. Mittal, A., Moorthy, A.K., Bovik, A.C.: No-reference image quality assessment in the spatial domain. IEEE TIP (2012) [4](#)
32. Mittal, A., Moorthy, A.K., Bovik, A.C.: No-reference image quality assessment in the spatial domain. IEEE TIP (2022) [4](#)
33. Mittal, A., Soundararajan, R., Bovik, A.C.: Making a “completely blind” image quality analyzer. IEEE Sign. Process. Letters (2013) [4](#)
34. Moorthy, A.K., Bovik, A.C.: A two-step framework for constructing blind image quality indices. IEEE Sign. Process. Letters (2010) [4](#)
35. Moorthy, A.K., Bovik, A.C.: Blind image quality assessment: From natural scene statistics to perceptual quality. IEEE TIP (2011) [4](#)
36. Openai: Gpt-4 technical report. arXiv preprint arXiv:2303.08774 (2023) [2](#), [3](#), [4](#), [5](#), [19](#)
37. OpenAI: GPT-4V(ision) system card. <https://openai.com/research/gpt-4v-system-card> (2023) [3](#), [4](#), [13](#), [25](#)
38. Ouyang, L., Wu, J., Jiang, X., Almeida, D., Wainwright, C., Mishkin, P., Zhang, C., Agarwal, S., Slama, K., Ray, A., et al.: Training language models to follow instructions with human feedback. In: NeurIPS (2022) [6](#), [9](#)
39. Pan, D., Shi, P., Hou, M., Ying, Z., Fu, S., Zhang, Y.: Blind predicting similar quality map for image quality assessment. In: CVPR (2018) [4](#)
40. Ponomarenko, N., Jin, L., Ieremeiev, O., Lukin, V., Egiazarian, K., Astola, J., Vozel, B., Chehdi, K., Carli, M., Battisti, F., et al.: Image database tid2013: Peculiarities, results and perspectives. Signal processing: Image communication (2015) [3](#), [5](#), [6](#)
41. Ponomarenko, N., Jin, L., Ieremeiev, O., Lukin, V., Egiazarian, K., Astola, J., Vozel, B., Chehdi, K., Carli, M., Battisti, F., et al.: Image database tid2013: Peculiarities, results and perspectives. Signal processing: Image communication (2015) [11](#)
42. Ponomarenko, N., Lukin, V., Zelensky, A., Egiazarian, K., Carli, M., Battisti, F.: Tid2008-a database for evaluation of full-reference visual quality assessment metrics. Advances of modern radioelectronics (2009) [3](#)
43. Prashnani, E., Cai, H., Mostofi, Y., Sen, P.: Pieapp: Perceptual image-error assessment through pairwise preference. In: CVPR (2018) [1](#), [2](#), [3](#), [4](#), [6](#), [10](#), [11](#)
44. Radford, A., Kim, J.W., Hallacy, C., Ramesh, A., Goh, G., Agarwal, S., Sastry, G., Askell, A., Mishkin, P., Clark, J., et al.: Learning transferable visual models from natural language supervision. In: ICML (2021) [8](#), [20](#)
45. Saad, M.A., Bovik, A.C., Charrier, C.: Blind image quality assessment: A natural scene statistics approach in the dct domain. IEEE TIP (2012) [4](#)
46. Sheikh, H.R., Bovik, A.C.: Image information and visual quality. IEEE TIP (2006) [4](#), [10](#), [11](#)
47. Su, S., Yan, Q., Zhu, Y., Zhang, C., Ge, X., Sun, J., Zhang, Y.: Blindly assess image quality in the wild guided by a self-adaptive hyper network. In: CVPR (2020) [4](#)
48. Sun, S., Yu, T., Xu, J., Zhou, W., Chen, Z.: GraphIQA: Learning distortion graph representations for blind image quality assessment. IEEE TMM (2022) [4](#)

49. Sun, W., Zhou, F., Liao, Q.: Mdid: A multiply distorted image database for image quality assessment. *Pattern Recognition* (2017) [11](#)
50. Tang, H., Joshi, N., Kapoor, A.: Learning a blind measure of perceptual image quality. In: *CVPR* (2011) [4](#)
51. Touvron, H., Lavril, T., Izacard, G., Martinet, X., Lachaux, M.A., Lacroix, T., Rozière, B., Goyal, N., Hambro, E., Azhar, F., et al.: Llama: Open and efficient foundation language models. *arXiv preprint arXiv:2302.13971* (2023) [2](#)
52. Touvron, H., Martin, L., Stone, K., Albert, P., Almahairi, A., Babaei, Y., Bashlykov, N., Batra, S., Bhargava, P., Bhosale, S., et al.: Llama 2: Open foundation and fine-tuned chat models. *arXiv preprint arXiv:2307.09288* (2023) [6](#), [8](#), [10](#), [20](#)
53. Tsimpoukelli, M., Menick, J.L., Cabi, S., Eslami, S., Vinyals, O., Hill, F.: Multi-modal few-shot learning with frozen language models. In: *NeurIPS* (2021) [4](#)
54. Wang, J., Chan, K.C., Loy, C.C.: Exploring clip for assessing the look and feel of images. In: *AAAI* (2023) [4](#)
55. Wang, Z., Bovik, A.C., Sheikh, H.R., Simoncelli, E.P.: Image quality assessment: from error visibility to structural similarity. *IEEE TIP* (2004) [1](#), [2](#), [4](#), [10](#), [11](#)
56. Wu, H., Zhang, Z., Zhang, E., Chen, C., Liao, L., Wang, A., Li, C., Sun, W., Yan, Q., Zhai, G., et al.: Q-bench: A benchmark for general-purpose foundation models on low-level vision. *arXiv preprint arXiv:2309.14181* (2023) [4](#)
57. Wu, H., Zhang, Z., Zhang, E., Chen, C., Liao, L., Wang, A., Xu, K., Li, C., Hou, J., Zhai, G., et al.: Q-instruct: Improving low-level visual abilities for multi-modality foundation models. *arXiv preprint arXiv:2311.06783* (2023) [4](#)
58. Wu, H., Zhang, Z., Zhang, W., Chen, C., Liao, L., Li, C., Gao, Y., Wang, A., Zhang, E., Sun, W., et al.: Q-align: Teaching llms for visual scoring via discrete text-defined levels. *arXiv preprint arXiv:2312.17090* (2023) [4](#)
59. Ye, Q., Xu, H., Xu, G., Ye, J., Yan, M., Zhou, Y., Wang, J., Hu, A., Shi, P., Shi, Y., et al.: mplug-owl: Modularization empowers large language models with multimodality. *arXiv preprint arXiv:2304.14178* (2023) [4](#)
60. Yin, G., Wang, W., Yuan, Z., Han, C., Ji, W., Sun, S., Wang, C.: Content-variant reference image quality assessment via knowledge distillation. In: *AAAI* (2022) [4](#)
61. Yin, Z., Wang, J., Cao, J., Shi, Z., Liu, D., Li, M., Sheng, L., Bai, L., Huang, X., Wang, Z., et al.: Lamm: Language-assisted multi-modal instruction-tuning dataset, framework, and benchmark. *arXiv preprint arXiv:2306.06687* (2023) [3](#), [4](#), [6](#), [9](#), [10](#), [11](#), [12](#), [23](#)
62. Zhang, L., Zhang, L., Mou, X., Zhang, D.: FSIM: A feature similarity index for image quality assessment. *IEEE TIP* (2011) [4](#), [10](#), [11](#)
63. Zhang, R., Han, J., Zhou, A., Hu, X., Yan, S., Lu, P., Li, H., Gao, P., Qiao, Y.: Llama-adapter: Efficient fine-tuning of language models with zero-init attention. *arXiv preprint arXiv:2303.16199* (2023) [4](#)
64. Zhang, R., Isola, P., Efros, A.A., Shechtman, E., Wang, O.: The unreasonable effectiveness of deep features as a perceptual metric. In: *CVPR* (2018) [1](#), [2](#), [3](#), [4](#), [6](#), [8](#), [9](#), [10](#), [11](#), [14](#), [20](#), [22](#), [24](#)
65. Zhang, W., Li, D., Ma, C., Zhai, G., Yang, X., Ma, K.: Continual learning for blind image quality assessment. *IEEE TPAMI* (2022) [4](#)
66. Zhang, W., Zhai, G., Wei, Y., Yang, X., Ma, K.: Blind image quality assessment via vision-language correspondence: A multitask learning perspective. In: *CVPR* (2023) [4](#)
67. Zhao, H., Cai, Z., Si, S., Ma, X., An, K., Chen, L., Liu, Z., Wang, S., Han, W., Chang, B.: Mmicl: Empowering vision-language model with multi-modal in-context learning. *arXiv preprint arXiv:2309.07915* (2023) [4](#), [9](#)

68. Zheng, H., Fu, J., Zeng, Y., Zha, Z.J., Luo, J.: Learning conditional knowledge distillation for degraded-reference image quality assessment. ICCV (2021) 4
69. Zhou, W., Wang, Z.: Quality assessment of image super-resolution: Balancing deterministic and statistical fidelity. In: ACM MM (2022) 4
70. Zhu, D., Chen, J., Shen, X., Li, X., Elhoseiny, M.: MiniGPT-4: Enhancing vision-language understanding with advanced large language models. arXiv preprint arXiv:2304.10592 (2023) 2, 3, 4, 8, 9, 11, 12
71. Zhu, H., Li, L., Wu, J., Dong, W., Shi, G.: MetaIQA: deep meta-learning for no-reference image quality assessment. In: CVPR (2020) 4

Appendix

A1 Overview

This *Appendix* is structured as follows. Dataset details are described in Sec. A2, followed by the methodology details in Sec. A3. Sec. A4 provides additional ablation studies. More quantitative results, qualitative results, and failure cases are presented in Sec. A5.

A2 Dataset Details

In this section, we provide additional descriptions and statistics of the introduced M-BAPPS dataset.

In-context learning for response generation. As detailed in the main paper, GPT-4 [36] is employed to convert human-annotated questionnaire options into a natural language paragraph. Yet, GPT-4 tends to produce responses that are overly verbose and potentially misleading. To mitigate this, we supply GPT-4 with two human-written examples to align the generated responses with a consistent writing style. Empirically, in-context learning effectively resolves these issues, yielding high-quality responses.

Questions in the question set. We show various question examples in the qualitative results of Task-1 (*quality description*, Fig. A8 & A9), Task-2 (*quality comparison*, Fig. A10 & A11), and Task-3 (*comparison reasoning*, Fig. A12, A13, & A14). This corroborates that users may express similar questions in different sentences, as discussed in the main paper.

Statistics of the response length in our M-BAPPS dataset are illustrated in Tab. A1. We present metrics on both word count and string length. For the evaluation of Task-2 (*quality comparison*), only the bi-classification ground-truth is utilized, so there is no need for statistics of the validation set. The distribution of word length in our M-BAPPS dataset is depicted in Fig. A1.

Statistics of questionnaire options are presented in Fig. A2 and Fig. A3. As detailed in the main paper, when annotating, annotators first complete a carefully designed questionnaire. Here we provide statistical breakdowns of the questionnaire’s options. Texture-related option statistics are outlined in Fig. A2.

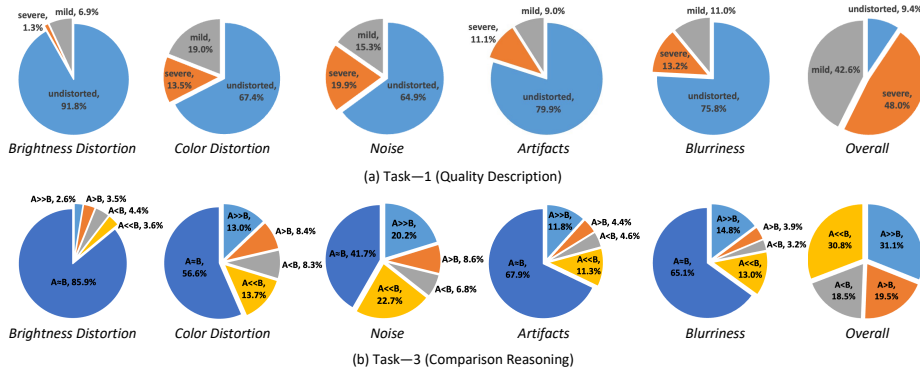


Fig. A3: Statistics of distortion-related options in the questionnaire with respect to (a) Task-1 (*quality description*) and (b) Task-3 (*comparison reasoning*). Note that there is no questionnaire for Task-2 (*quality comparison*), hence no statistic is required.

as 16. There are 32 attention layers in the LLM in total. In each attention layer, the projection weights of “query”, “key”, “value”, and “output” are adjusted using two delta parameters with the shape of 4096×16 and 16×4096 , respectively.

A3.2 Metrics

Accuracy. Our DepictQA could directly output binary classification results (*i.e.*, Image A or Image B is better) using the short answer prompt for accuracy computation. For other MLLMs, we deploy GPT-3.5 to convert varied textual comparison results into binary classification results for accuracy computation. Upon gathering approximately 10k textual comparison results and their binary classifications, we train a BERT [9] model, achieving 97.5% agreement with GPT-3.5 in the test dataset.

GPT4-score. To compute the GPT4-score for one response, we input GPT-4 with the following contents: “context”, “question”, “answer_1”, “answer_2”, and “instruction”. The “instruction” directs GPT-4 to assess two answers (“answer_1” and “answer_2”) to the same “question” using the “context” knowledge, and then rate each answer on a scale of [0, 10]. The “context” contains all information in the human-labeled questionnaire, which is the correct knowledge for GPT-4 to evaluate answers. The “question” refers to the quality-related question posed to the MLLMs. The “answer_1” is actually the ground-truth response, which is labeled by human-evaluators. The “answer_2” is the response of the MLLM to be evaluated. Then, the score of “answer_2” (*i.e.*, the MLLM to be evaluated) relevant to “answer_1” (*i.e.*, the ground-truth) serves as the GPT4-score of “answer_2”. We calculate the final metric by averaging the scores across all samples. As discussed in the main paper, the GPT4-score tends to be overly generous for low-quality responses, resulting in inflated scores. One example is shown in Fig. A5, where a fully wrong response receives a GPT4-score of 66.7%.

Reasonable rate evaluated by humans. Human evaluators are requested to label each response as either reasonable or unreasonable, based on the pro-

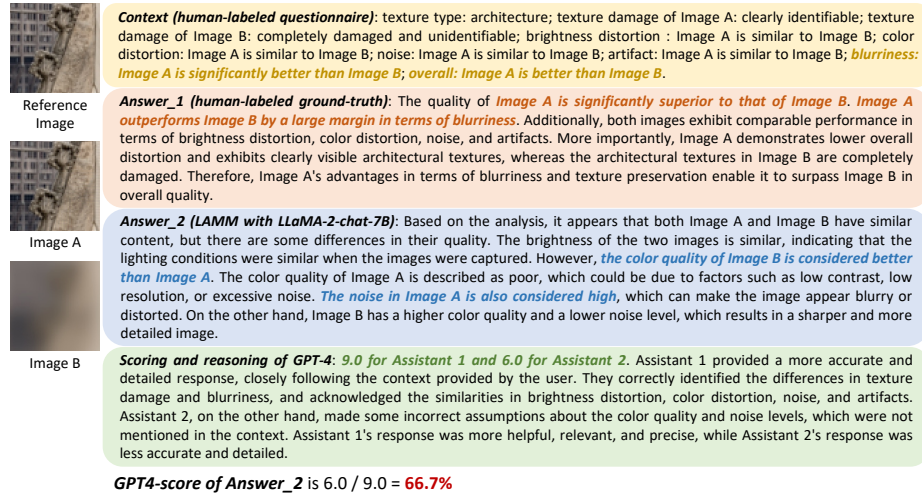


Fig. A5: GPT4-score sometimes exhibits excessive confidence in low-quality responses, though widely adopted as metrics in MLLMs [8, 28]. In this case, a fully wrong response still receives a GPT4-score of 66.7%.

Table A2: Ablation studies. (a) Ablation studies regarding **LoRA rank** with accuracy metric on BAPPS benchmark [64]. (b) Comparison of **different methods to distinguish multiple images**. The comparison ability is assessed by accuracy within Traditional / CNN categories. The reasoning ability is evaluated by reasonable rate. The performance of image embedding and unique projector is obviously inferior to unique tag.

(a) Different LoRA ranks.						(b) Various methods to distinguish multiple images.		
LoRA Rank	8	12	16	24	32	Method	Comparison	Reasoning
Traditional	fail	79.7	80.0	79.6	80.5	Image Embedding	67.0 / 66.9	26.0
CNN	fail	83.9	83.8	84.0	83.8	Unique Projector	75.1 / 77.2	40.0
Average	fail	81.8	81.9	81.8	82.1	Unique Tag	80.0 / 83.8	53.0

vided images and corresponding responses. One “reasonable” response should adhere to three criteria. (1) The response must accurately identify the most important quality issue that directly influences the comparison result. (2) The response should avoid serious false positive distortions conflicting with human evaluation. (3) The response’s description, reasoning, and conclusion should align closely. Minor errors not violating these three rules are permissible.

A4 Ablation Studies

Influences of LoRA rank are illustrated in Tab. A2a. When LoRA rank is too small (*e.g.*, 8), the training process diverges. When the training process converges with larger LoRA rank (*e.g.*, 12, 16, 24, and 32), our DepictQA is insensitive to this hyper-parameter. The default choice of LoRA rank is 16.

Different methods to distinguish multiple images. In addition to the unique tag method introduced in the main paper, we investigate alternative strategies for managing multiple images. (1) Image embedding. We add a trainable embedding to visual tokens for each image type. In *comparison* and *reasoning* tasks, distinct embeddings are assigned to the reference image, Image A, and Image B. For the *description* task, the embeddings for the reference image and Image A are added to the tokens of the reference images and distorted images, respectively. (2) Unique image projector. We utilize unique image projectors for varied image categories. These projectors are specifically initialized for the reference image, Image A, and Image B in *comparison* and *reasoning* tasks. In the *description* task, only projectors for the reference image and Image A are employed. The experimental results are illustrated in Tab. A2b. The performance of image embedding and unique projector is obviously inferior to unique tag. We suspect that the reason could be that changing the visual tokens differently for various images may confuse the model.

Comparison of global feature and local feature map. The ViT-L/14 image encoder produces a singular global feature token and a multi-token local feature map. Either can function as visual tokens of the MLLM. We analyze the performance differences between the global feature and local feature map in Tab. A3. The global feature demonstrates lesser effectiveness than the local feature map, particularly in reasoning tasks. This disparity might come from the global feature’s singular visual token, which restricts the amount of information conveyed.

Impacts of content description data on texture diversity. Incorporating external content description data, specifically the Detailed Description Dataset in [61], stably enhances the performance, as discussed in the main paper. Training with content description data also enriches the diversity of texture types recognized, even beyond the pre-defined categories in our training set, as depicted in Fig. A6. For instance, in the last two examples in Fig. A6, though the texture types of “trees” and “flowers” are usually annotated as “plants” in the training set, we still correctly predict these fine-grained texture types.

Table A3: Comparison of global feature and local feature map. The comparison ability is assessed by accuracy within Traditional / CNN categories. The reasoning ability is evaluated by reasonable rate. Local feature map surpasses global feature obviously.

	Comparison	Reasoning
Global Feature	76.7 / 80.8	34.0
Local Feature Map	80.0 / 83.8	53.0

	Texture Type			
Image				
Prediction	Mountains †	Jeans †	Trees †	Flowers †
Closest Annotation in Training Set	Ground	Fabrics	Plants	Plants

† Beyond our pre-defined texture types in the training set

Fig. A6: Training with the content description data improves the diversity of texture types in responses, which even beyond our pre-defined texture types in training set.

A5 More Results

A5.1 More Results of Quality Description

Qualitative results of quality description are illustrated in Fig. A8 and A9. We sample these results from:

- Different distortions. *e.g.*, *blurriness* in A8a & A9c, *noise* in A8c & A9e, *color distortion* in A8d & A9d.
- Various contents. *e.g.*, *plants* in A8c & A8e, *architectures* in A8d & A9b, *people* in A8f.
- Diverse distortion degrees. *e.g.*, *severe* in A8a & A9d, *mild* in A8b, A8d, & A8e, *no distortion* in A8f & A9b.

A5.2 More Results of Quality Comparison

Consistency with the tendencies of human annotators.

The ground-truth scores in the BAPPS dataset [64] represent the proportion of annotators favoring Image B. In the validation set of BAPPS, there are 5 annotators in total, so the value of the ground-truth score varies across [0, 0.2, 0.4, 0.6, 0.8, 1.0]. As shown in Tab. A4, when we exclude the samples with high label uncertainty in the BAPPS dataset, the comparison accuracy of our DepictQA improves significantly, indicating that our model behaves consistently with the tendencies of human annotators.

Table A4: Our DepictQA behaves consistently with the tendencies of human annotators. When excluding samples with high label uncertainty in BAPPS dataset [64], the comparison accuracy improves significantly.

Excluded Labels	\emptyset	{0.4, 0.6}	{0.2, 0.4, 0.6, 0.8}
Traditional	80.0	86.1	92.1
CNN	83.8	89.4	94.5
Average	81.9	87.8	93.3

Qualitative results of quality comparison are illustrated in Fig. A10 (without short answer prompt) and A11 (with short answer prompt). DepictQA aligns closely with human judgments under the circumstances:

- Different types of distortions. *e.g.*, *blurriness* in A11b & A11c, *noise* in A10a & A10b, *color distortion* in A10g & A11f, *artifacts* in A11a & A11d.
- Different texture types. *e.g.*, *architectures* in A10a & A11c, *object edges* in A11f, *water surface* in A10b & A10f, *plants* in A10d & A11d.
- Both images suffering from severe distortions. *e.g.*, *color distortion* in A & *blurriness* in B in A10d, *noise* in A & *blurriness* in B in A11c.

A5.3 More Results of Comparison Reasoning

Qualitative results of comparison reasoning are illustrated in Fig. A12, A13, and A14. Similar to Sec. A5.2, these samples are sampled from:

- Various categories of distortions. *e.g.*, *color distortion* in A12a & A12c, *blurriness* in A13c & A14a, *artifacts* in A14b & A14c, *noise* in A13a & A14d.



... The quality of Image B is significantly superior to that of Image A. Image A noticeably falls short in two key factors, *color distortion and artifacts* ...

Fig. A7: Visualization of the attention map. We visualize decoder attention weights between the **highlighted words** and the visual tokens. Our model focuses on relevant regions containing text-described distortions.

- Different image contents. *e.g.*, *sky and clouds* in A12b, *architectures* in A13a & A14c, *plants* in A12d & A13c.
- Both images with severe distortions. *e.g.*, *color distortion* in A & *blurriness* in B in A14a, *color distortion* in A & *noise* in B in A12c.

A5.4 Failure Cases

Failure cases of DepictQA in *quality description* and *comparison reasoning* tasks are presented in Fig. A15. (1) Fig. A15a and A15b show DepictQA incorrectly identifying distortion types, leading to wrong quality assessments in the quality description task. (2) In Fig. A15c, DepictQA mistakenly attributes the noise in Image A to Image B, resulting in an incorrect comparison result. As reflected in Fig. 4 in the main paper, the unique tag approach does not completely resolve the confusion issue. (3) In Fig. A15d, DepictQA fails to recognize an unusual distortion (*i.e.*, complete semantic content washout in Image B). This is primarily due to the absence of such distortions in the training set.

A5.5 More Results of GPT-4V

Qualitative results of GPT-4V [37] in *comparison reasoning* task are shown in Fig. A16. GPT-4V gives quite detailed comparison reasoning results, which is the main reason for its excellent GPT4-score (see Tab. 4 in the main paper).

Failure cases of GPT-4V in *comparison reasoning* task are given in Fig. A17. Despite GPT-4V providing detailed reasoning texts, it mistakenly describes distortions, texture damages, and comparison results.

A5.6 Extension

Potential for distortion localization. In Fig. A7, we visualize decoder attention weights between the texts describing distortions and the visual tokens. Our model focuses on regions containing text-described distortions. This invites our future research into precise distortion localization based on textual outputs.

Reference:  Image: 

What criteria are you using to assess the overall quality of the image, and can you explain your assessment in detail?

The overall quality of this image is **severely compromised**, primarily due to **the issue of blurriness**. Although the **distortions in brightness, color, noise, and artifacts are minimal**, the problem of blurriness significantly reduces the overall clarity of the image. Moreover, **the texture features of the image are completely damaged**, making it impossible to discern the texture information originally contained in the image. Therefore, it can be concluded that blurriness is the main reason for the decline in the overall quality and texture damage of this image.

Reference:  Image: 

How would you rate the quality of the image, and what specific elements contribute to your assessment?

The quality of this image is quite **good**, with **only minor issues**. **The brightness and color are well-balanced**, and there are **no significant noise or artifacts**, indicating a high level of image quality. However, the image's clarity is **slightly reduced, possibly due to blurring**, which impacts the overall quality of the image to a certain extent. Overall, the image distortion is minimal, and the texture features, especially **the texture of the object edges, can still be clearly identified**. Therefore, the image quality is generally good, with the main issue being the slight blurring, which may impact the image's clarity, but not severely.

Reference:  Image: 

Could you please analyze the quality of the image, and then elaborate on your assessment?

The overall quality of this image is **severely compromised**, primarily due to **the significant noise** within the image, which drastically reduces its clarity and results in poor visual effects. Although there are **no apparent distortions in brightness and color**, and **the degree of artifacts and blurring remains at a low level**, these factors cannot offset the damage that noise has done to the image quality. Additionally, the damage to the image's texture is also severe, particularly **the texture of the plants, which is now entirely unrecognizable**, demonstrating the destructive impact of noise on image quality. Therefore, it can be definitively concluded that the quality of this image is severely affected, with noise being the primary factor leading to this outcome.

Reference:  Image: 

In your opinion, what are the strengths and weaknesses of the image in terms of quality, and why?

The overall quality of this image is **good**, with **only minor distortions**. Among the five evaluation factors, **brightness, noise, artifacts, and blurring have virtually no distortion**, indicating that the image's brightness, clarity, authenticity, and sharpness are well preserved. However, there is **a certain degree of distortion in terms of color**. Nevertheless, due to the good performance of the other factors, the overall distortion of the image is still considered minor. In terms of texture, **the texture of architecture is clearly visible and is not greatly affected by color distortion**. Therefore, I conclude that despite minor color distortion, the overall quality and texture quality of this image still remain at a high level.

Reference:  Image: 

Assess the image's quality with a critical eye, highlighting both strengths and areas for improvement.

The overall quality of this image is **acceptable**, but there are some issues related to **blur and noise**. Although **the distortion in terms of brightness, color, and artifacts is minimal**, the slight blur and noise have somewhat impacted the image quality. This is also reflected in the evaluation of overall distortion, where the overall distortion level of this image is slightly higher than that of the reference image. Moreover, **the blur and noise have somewhat impacted the recognition of the plant texture**. The degree of texture damage is barely recognizable. Overall, although the image quality is acceptable, the slight blur and noise have impacted the image texture, resulting in a certain degree of loss in image quality.

Reference:  Image: 

Evaluate the overall quality of the image and provide a comprehensive explanation of your assessment.

The image has **excellent performance** in terms of quality assessment, **with hardly any noticeable distortion**. The level of distortion is minimal, nearly negligible, indicating that the image quality is high and nearly perfect. The texture features of the image are also well preserved, **with the facial texture clearly visible, and the degree of texture damage is extremely low**. This suggests that the image has been created using advanced image processing technology, with virtually no artifacts, and the processing is done quite effectively. Overall, the image has high quality, with almost no distortion, especially in terms of texture, where the original features are well preserved, making it an outstanding image.

Fig. A8: Qualitative results of DepictQA on quality description task. Our DepictQA could clearly identify **distortions** and **texture damages**, then weigh the impacts of various aspects to draw the final **conclusion**.

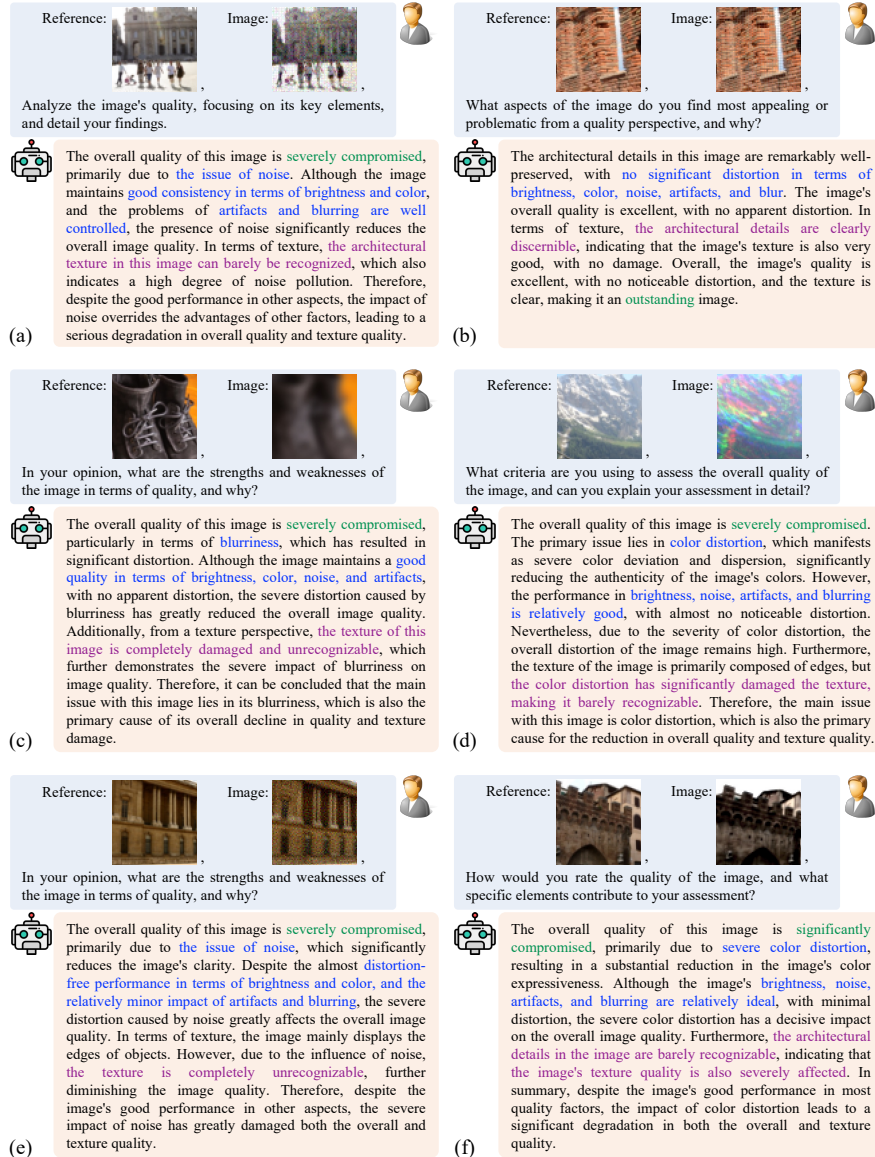


Fig. A9: Qualitative results of DepictQA on quality description task. Our DepictQA could clearly identify **distortions** and **texture damages**, then weigh the impacts of various aspects to draw the final **conclusion**.

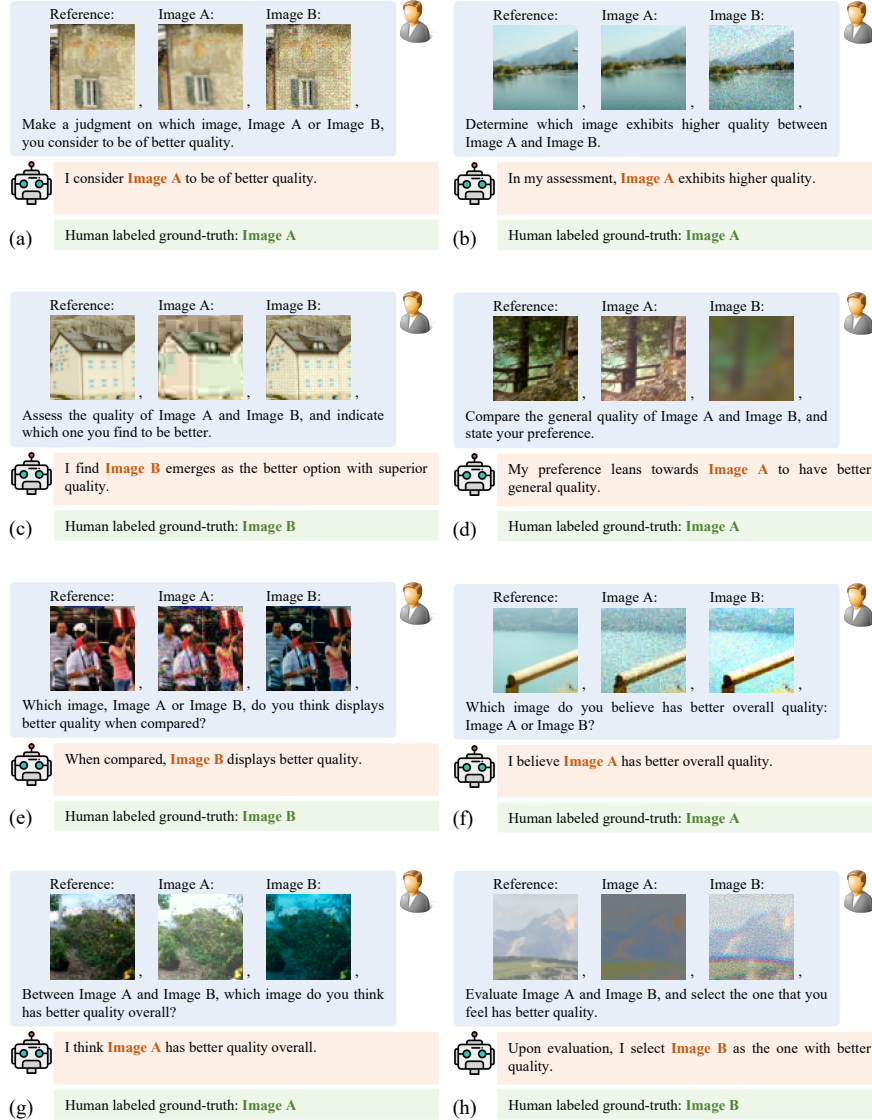


Fig. A10: Qualitative results of DepictQA on quality comparison task (without short answer prompt). Our DepictQA aligns quite well with human judgments.

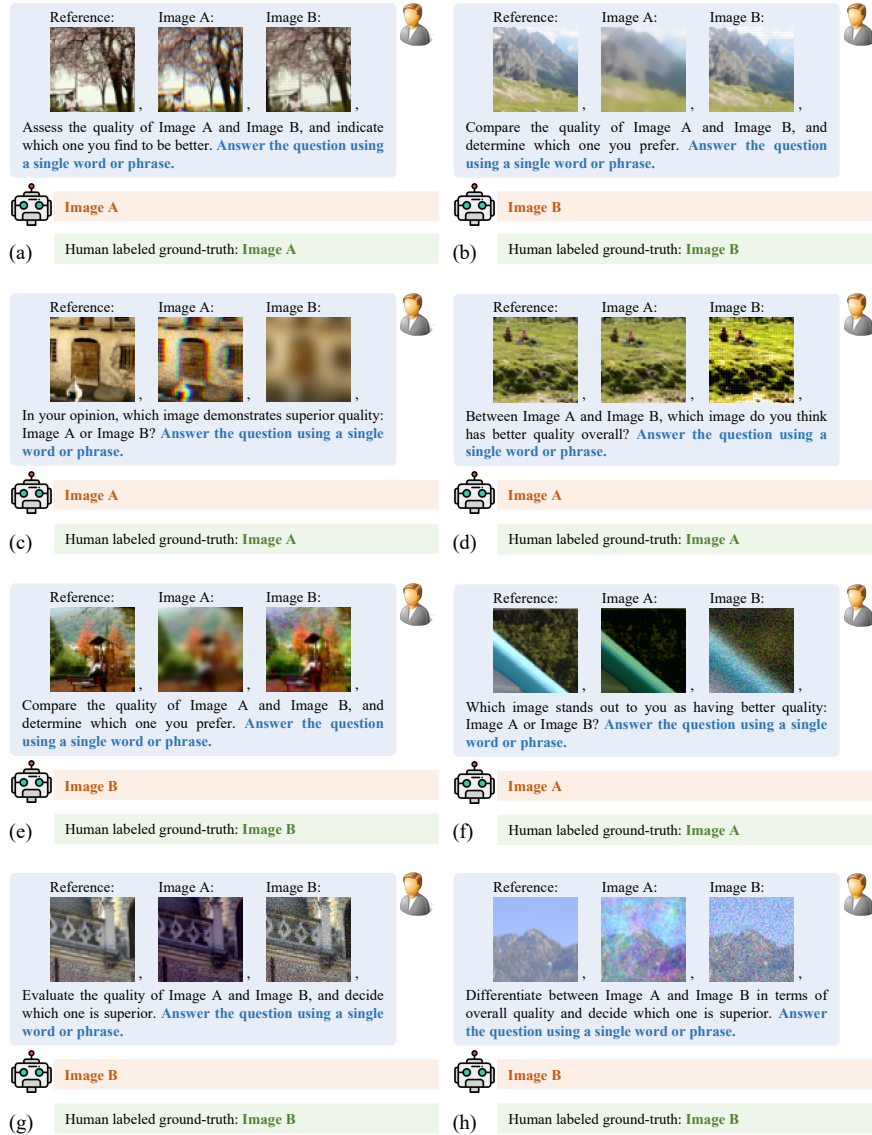


Fig. A11: Qualitative results of DepictQA on quality comparison task (with short answer prompt). Our DepictQA aligns quite well with human judgments.



Fig. A12: Qualitative results of DepictQA on comparison reasoning task. Our DepictQA could comparatively identify distortions, then weigh the impacts of these distortions to the texture damages, and finally draw the final comparison conclusion.



Fig. A13: Qualitative results of DepictQA on comparison reasoning task. Our DepictQA could comparatively identify distortions, then weigh the impacts of these distortions to the texture damages, and finally draw the final comparison conclusion.



Fig. A14: Qualitative results of DepictQA on comparison reasoning task. Our DepictQA could comparatively identify **distortions**, then weigh the impacts of these distortions to the **texture damages**, and finally draw the final **comparison conclusion**.

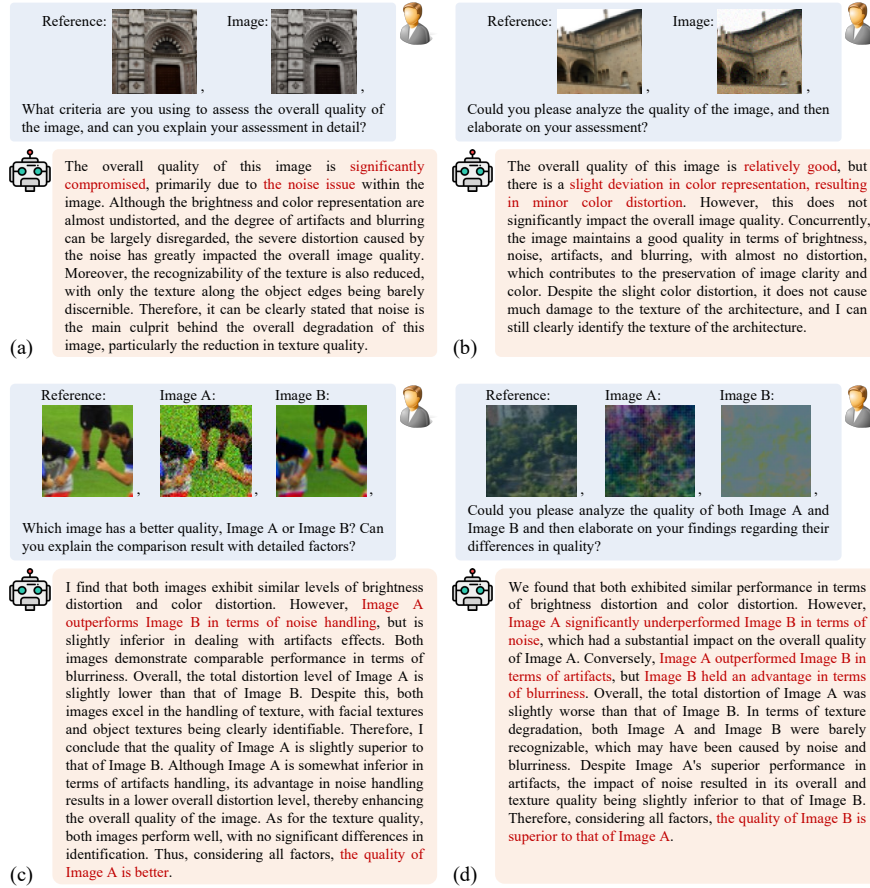


Fig. A15: Failure cases of DepictQA in (a)(b) quality description task and (c)(d) comparison reasoning task.



Fig. A16: Qualitative results of GPT-4V in comparison reasoning task.

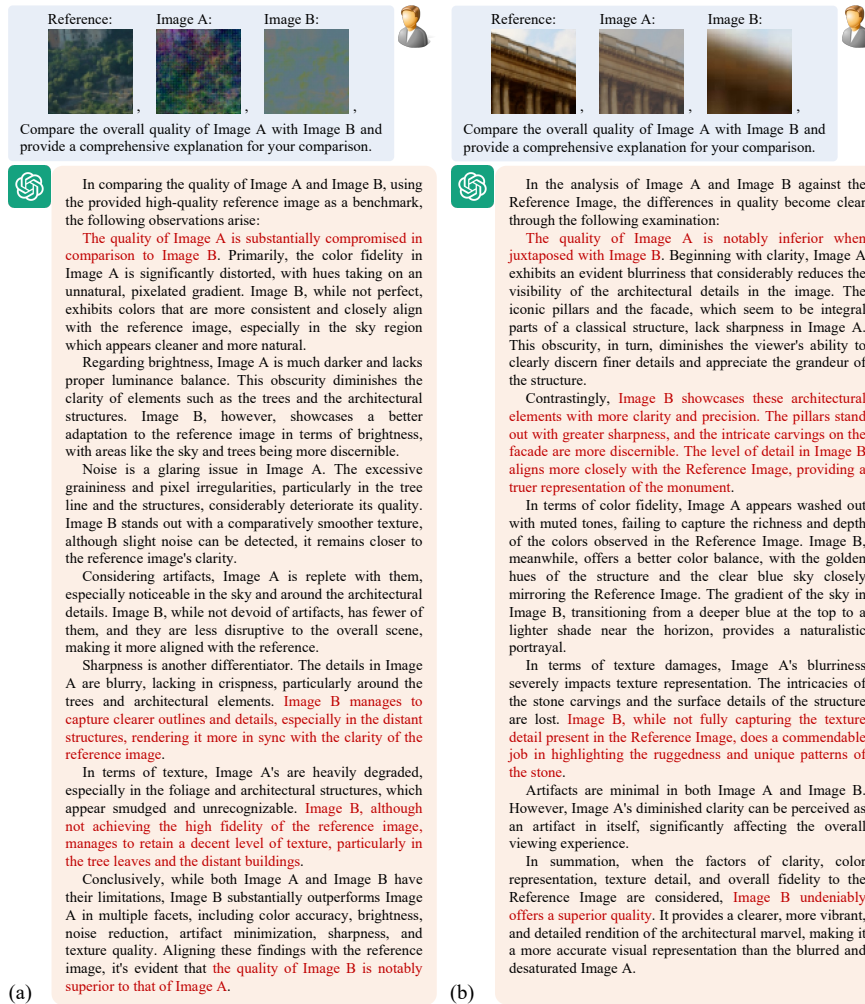


Fig. A17: Failure cases of GPT-4V in comparison reasoning task.